

Sustainability in Electric Transportation: Minimizing Transportation Energy

1st Peter H. Bauer
Department of Electrical Engineering
University of Notre Dame
Notre Dame, USA
pbauer@nd.edu

2nd Eduardo F. Mello
Department of Electrical Engineering
University of Notre Dame
Notre Dame, USA
emello@nd.edu

Abstract—A variety of energy-saving concepts that exploit the special characteristics of electric drives are introduced. The confluence of three emerging concepts in transportation, namely electric drives, autonomous driving, and networked vehicles, enables the optimization of transportation efficiency in a way that drastically changes modern transportation, especially for passenger and commercial road vehicles. The paper addresses both, urban as well as highway driving situations and the associated optimization problems. It is shown that if the only term in the cost function is transportation energy, and all other conditions are formulated as constraints, quite substantial energy cost reductions are possible. Exploiting weather and environmental conditions is another important topic that is analyzed. The paper illustrates key ideas via several simulation examples.

Keywords—Electric drives, autonomous vehicles, energy efficiency, optimization, speed profiles, environmental factors

I. INTRODUCTION

Worldwide, a substantial part of emissions and consumption of fossil fuels originates from transportation [1]. Moving to alternative non-fossil fuel based transportation is a promising avenue, especially if the energy comes from solar, wind, nuclear or hydropower. In the future, the usage of electric drives can play a major role in transportation applications, especially in densely populated urban areas [2], even though acceptance is slower than originally expected. There are immense opportunities in the improvement of transport efficiency when one combines electric drives with autonomous operations and networked vehicles with situational traffic awareness. This paper outlines some of the opportunities arising from the combined application of these three concepts.

There has been a vast amount of work in the area of “green driving”, i.e., optimizing efficiency by changing the way vehicles are driven [1]–[5]. This includes choosing the engine operating point in a particular way, minimizing speed changes, communicating with the traffic infrastructure to minimize the number of stops, just to name a few. Optimizing vehicle operating points only works if the driver is willing and able to execute the optimal algorithm or at least the set of rules that ensure efficiency gains. Therein lies a big opportunity for future vehicles: Self-driving capability ensures that an exact execution of a desired speed trajectory

can be performed with close to zero error, and the networked vehicle concept enables transmission of situational traffic awareness data, see Fig. 1. We will illustrate in this paper, that applying these two concepts to electric drives can generate enormous energy savings. This is due to some special properties of electric drives that will be explained in the following sections.

This paper is structured as follows: In section II, the fundamental models for power flow and optimization are introduced. Section III discusses and illustrates the sensitivity of e-drives to environmental and weather conditions, which can be exploited to reduce energy consumption, as shown in section IV. Section V addresses the problem of energy optimal stop to stop trajectory as they occur in urban and suburban situations. Urban e-platoons and their potential for efficiency optimization are presented in section VI. Finally, section VII presents conclusions and an outlook on how to realize the presented concepts over time.

II. POWERTRAIN AND OPTIMIZATION MODELS

Two types of models are presented in this section: A powerflow model for characterizing energy expenditures and several optimization models to be used later for minimizing transportation energy at the source.

A. Energy and Power Model

The powerflow in the electric powertrain and the balance of forces acting on the vehicle are shown in Fig. 2. Based on [6], the corresponding power balance equation, without hill-climbing, is shown in (1). The power at the wheel is denoted as P_{wheel} , the mass, speed, acceleration, frontal drag coefficient, and cross-sectional area of the vehicle are denoted by m , $v(t)$, $\dot{v}(t)$, C_d , and A , respectively. The vehicle mass also models and includes the driveline inertia, which appears as a constant additional mass contribution, i.e., a single gear transmission is assumed [7]. The air density is

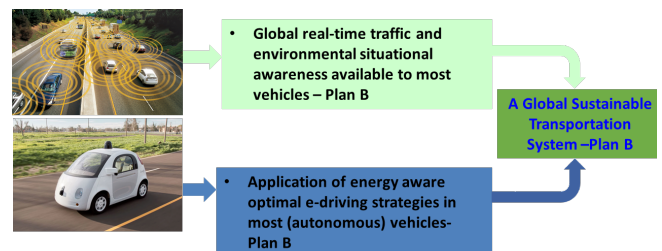


Fig. 1. The confluence of autonomous, electric and networked (situational aware) vehicles.

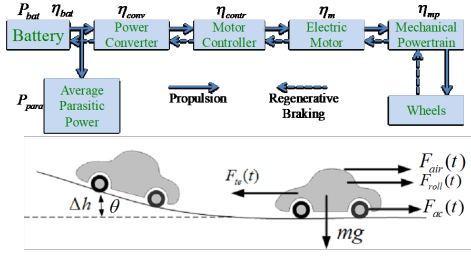


Fig. 2. Powerflow model in an electric drive.

denoted by ρ , f_r is the coefficient of rolling resistance, and g is the gravitational acceleration.

$$P_{wheel}(t) = mv(t)\dot{v}(t) + \frac{1}{2}C_dA\rho v(t)^3 + mgf_r v(t) \quad (1)$$

The power flow equation for forward motion and reverse power flow, is given by (2):

$$P_{bat}(t) = \begin{cases} \eta_{frw}(T, \omega)^{-1} P_{wheel}(t) & \text{for } P_{wheel} \geq 0 \\ \eta_{reg}(T, \omega) P_{wheel}(t) & \text{for } P_{wheel} < 0 \end{cases} \quad (2)$$

where $P_{bat}(t)$ is the power at the battery, $\eta_{frw}(T, \omega)$ is the vehicle's efficiency for forward power flow, $\eta_{reg}(T, \omega)$ for reverse power flow, T is the torque of the motor, and ω its the rotational speed. These efficiencies represent the complete powertrain efficiency, including the mechanical drivetrain, and battery efficiency which, as shown in [8], have little variations under different operating conditions.

B. The Optimization Models

Fig. 3 illustrates the two fundamental optimization formulations; the minimization of energy with time as a constraint and its dual case, i.e., minimization of time with energy as a constraint. In the depicted formulation, E_0 and t_0 are energy and time constraints respectively. v_{ll} and v_{lu} refer to additional speed constraints.

As shown in [9], in order to minimize the energy consumption of an EV for a specific traffic segment with a desired average speed one can formulate the following optimization problem. Constraints are average speed v_{avg} , covered distance x , acceleration \dot{v}_{max} , and jerk \ddot{v}_{max} limits:

$$\begin{aligned} \text{minimize}_{v(t)} \quad & \int_0^{t_f} P_{bat}(\tau) d\tau, \quad s.t. \quad \int_0^{t_f} v(\tau) d\tau = x \\ & X/t_f = v_{avg} \\ & \dot{v}_{min} < \dot{v}(t) < \dot{v}_{max} \\ & \ddot{v}_{min} < \ddot{v}(t) < \ddot{v}_{max} \end{aligned} \quad (3)$$

where $P_{bat}(\tau)$ is given by (2), t_f is the total time of the optimization, \dot{v}_{min} and \dot{v}_{max} are the minimum and maximum acceptable acceleration values, and \ddot{v}_{min} and \ddot{v}_{max} are the minimum and maximum acceptable jerk values.

More constraints may have to be imposed, depending on

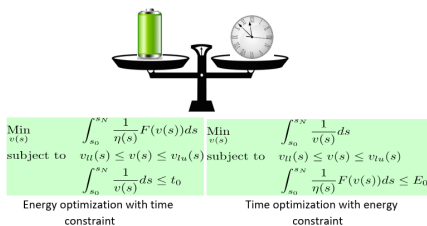


Fig. 3. Energy vs. time optimization.

the application. For example, speed boundary conditions, acceleration and jerk conditions all may play an important role in some of the considered optimization problems.

III. E-POWERTRAIN CHARACTERISTICS AND THEIR SENSITIVITY

Electric drives in many ways differ significantly from conventional powertrains. For the purpose of this analysis, we will concentrate on the efficiency as a function of torque and speed. To illustrate this point, consider Fig. 4 that depicts two efficiency maps, one for a conventional ICE and one for an electric drive. Two differences are apparent: The efficiency levels in an e-drive are significantly (two to three times) higher and they vary less as a function of torque and speed, i.e., e-drives usually show a large plateau of high efficiency whereas in conventional drives there usually is a very well defined efficiency peak or ridge. This also explains why for e-drives in certain operating conditions a constant or lumped efficiency model can provide fairly accurate results.

Next, we will show via a brief sensitivity analysis and examples, that e-drives show an unusually high sensitivity to external environmental factors. The sensitivity of the quantity P_{bat} with respect to a quantity x is defined by:

$$S_x = \lim_{\delta x \rightarrow 0} \frac{[P_{bat}(x + \delta x) - P_{bat}(x)]/P_{bat}}{\delta x/x} = \frac{\partial P_{bat}}{\partial x} \frac{x}{P_{bat}} \quad (4)$$

For the problem at hand, P_{bat} is battery power and x can be a variety of different variables such as wind speed ω , coefficient of rolling resistance f_r , parasitic power P_{para} or possibly temperature of the powertrain/batteries. The sensitivity depends on driving conditions and can vary widely depending on operating conditions. As an example, let us consider a Tesla Model S in two different situations, i.e., highway and urban conditions. The result depicted in Fig. 5 shows that energy sensitivity with respect to rolling resistance is much higher in urban driving than in highway conditions, whereas the opposite is true for the air drag term.

Also, parasitic power almost plays no role in highway driving whereas it is significant in urban environments. In

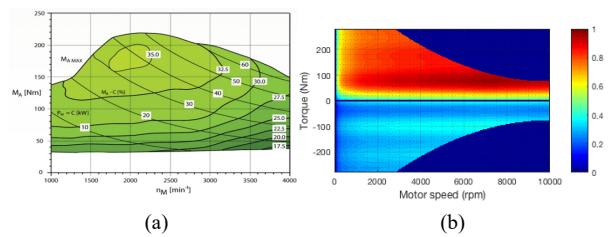


Fig. 4. Efficiency maps for an (a) ICE engine powertrain and an (b) electric drive.

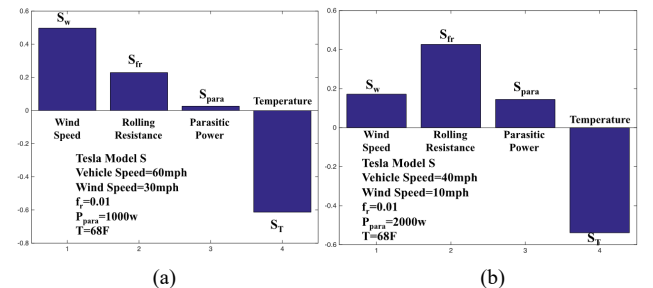


Fig. 5. Power sensitivity with respect to the different variables.

order to illustrate the role each of the energy components plays in a typical trip, consider the drive from South Bend, IN to Chicago, IL through the interstate 90. Using a mix of FTP 75 urban, highway and US 06, the total transportation energy at the battery was computed when one variable was changed at a time, i.e., wind speed and direction, rolling resistance, parasitic power, and temperature. The results obtained by varying the rolling resistance coefficient are shown in Fig. 6, the parasitic power in Fig. 7 and the wind speed and direction in Fig. 8. The most pronounced effects are of air drag and rolling resistance coefficient, which can easily change the nominal energy consumption for the trip (25KWh) by 20-30% depending on weather conditions. For example, consider the curves for a Nissan Leaf for westerly and easterly wind changes of 10m/s. The energy needed for the trip changes from 25KWh to 30KWh for westerly winds and from 25KWh to 22KWh for easterly winds of 10m/s. Similarly, comparing clear roads with a rolling resistance coefficient of 0.01 to wet, heavy snow conditions with a coefficient near 0.03, the energy consumption increases from 25KWh to approximately 40KWh.

IV. EXPLOITING ENVIRONMENTAL CONDITIONS

In light of the high sensitivity of e-drives to

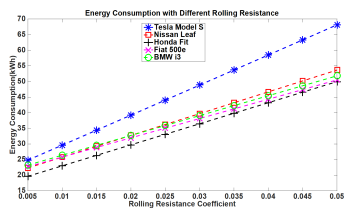


Fig. 6. Energy consumption as a function of rolling resistance coefficient for a trip from South Bend, IN to Chicago, IL.

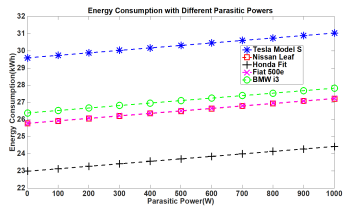


Fig. 7. Energy consumption as a function of parasitic power for a trip from South Bend, IN to Chicago, IL.

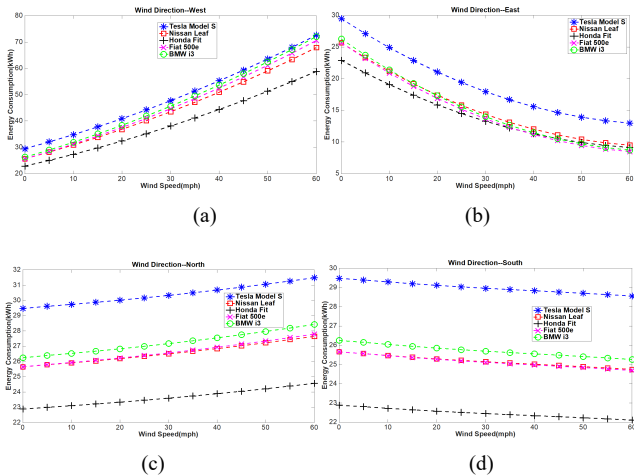


Fig. 8. Energy consumption as a function of wind speed and direction for a trip from South Bend, IN to Chicago, IL.

environmental factors, it makes sense to exploit these dependencies to boost efficiency. As an example, consider a vehicle that does a roundtrip from A to B and back to A. Assume there is a headwind when traveling from A to B and a tailwind from B to A. Then for a conventional drivetrain the fuel consumption differs little between the two drive segments assuming identical speeds, because in case of a headwind the torque increases (keeping speed the same) and thus both, power and the efficiency increase, while in the case of a tailwind power and efficiency are reduced, resulting in similar fuel consumption. Of course, this assumes that the engine does not operate at or near the efficiency maximum, which usually is the case. However, in the case of an e-drive, the efficiency in both directions stays approximately the same (due to the large efficiency plateau in the speed-torque diagram) and the trip portion with a headwind will see a higher energy expense than the portion with a tailwind. Therefore, one can exploit this dependency and adapt the speed with respect to environmental conditions, i.e., in this case by reducing the speed in case of a headwind and increasing it for a tailwind. Based on the results in the previous section, one can optimize transportation energy with respect to wind, rolling resistance coefficient, temperature, and parasitic power.

There are two basic optimization problems that can be formulated: (i) Minimizing energy with trip time as the constraint and (ii) minimizing trip time with energy as a constraint, which is the dual problem.

For the sake of brevity, we will only illustrate how to exploit the presence of different wind speeds along a trip. Similar approaches can be taken with respect to the other three quantities, even though the largest savings are obtained by exploiting wind speed fluctuations. Also, we will not consider the time minimization problem, since there are fewer applications. For details please refer to [10].

In [10], several different approaches were introduced that range from optimization with exactly known wind speed profiles to robust optimization where wind speeds are highly uncertain using an interval description. For the purpose of this paper, we limit the discussion to the deterministic case.

Consider the example of a trip that is divided into 50 drive segments and in each drive segment, the wind speed is constant. For the sake of simplicity, we assume the wind speed varies from segment to segment randomly and takes values between -10m/s to +10m/s in steps of 5m/s, i.e., possible values are -10, -5, 0, +5 and +10m/s.

Fig. 9 clearly the energy optimal speed trajectory. The average vehicle speed of 27m/s is maintained while adjusting the vehicle segment speed to the wind speed, i.e. vehicle speed is increased for tailwinds and reduced for headwinds.

Now consider Fig. 10 that shows two different routes,

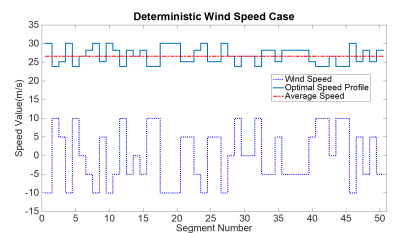


Fig. 9. Wind speed fluctuations and associated optimal vehicle speed variations.

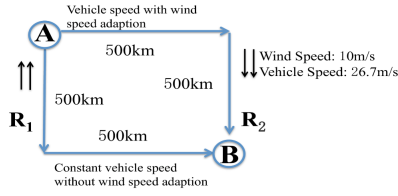


Fig. 10. Two routes with different weather conditions—a transportation energy comparison.

i.e., route R1 and route R2, both leading from A to B. In the vertical parts of the two routes, route R1 encounters a headwind while route R2 encounters a tailwind. On the horizontal portions of the trip, wind speed changes as shown in Fig. 9 and these changes are identical for both routes. The vehicle traveling that route is a 10ton truck with a frontal cross-sectional area of 8 square meters. The difference in energy consumption for the two route is fairly large, and route 2 offers a 37.7% energy advantage over route 1, most of which coming from the vertical trip components.

V. OPTIMAL STOP-TO-STOP TRAJECTORIES

Emissions and excessive energy usage are especially problematic in urban environments and worldwide, cities are trying to limit traffic and emissions in urban centers. For this reason, plug-in hybrids and purely battery electric vehicles are an attractive option since they can operate without emissions. Even in smart cities with intelligent traffic infrastructure and optimized traffic flow, city driving can be modeled as stop-to-stop traffic. Due to the special properties of electric drives, this type of driving environment is well suited for optimization of speed trajectories, i.e. trajectories that are energy optimal. In other words, given a drive segment length, boundary conditions, i.e., zero speed, and drive time (or equivalently average speed), there are infinitely many speed trajectories that satisfy the above mentioned conditions, but there is only one such trajectory that is energy optimal. What we will show in this section is that for short and medium-length segments, energy savings produced by the optimal trajectory relative to typical trajectories can be very large, sometimes exceeding 50%. Such high levels of energy savings have a multitude of effects, including significantly extended range, less stress on the power grid, less congestion at charging stations, and lower cost of electric transportation. Of course, if power comes from renewable energy sources, this also translates into lower emissions.

For all results presented we assume perfect situational awareness for each drive segment, i.e. typical accelerations, speed constraints, and segment length are known before each segment is started. We further assume, that the stop-to-stop segments in the FTP 75 urban cycle are typical and they are used as a reference and referred to as the “typical trajectory”.

A. Boundary Conditions and Constraints

The optimization problem is very similar to the problem stated in equation (3) in section II, i.e. we minimize transportation energy at the battery with a time constraint. However, additional constraints come from the fact that the speed at the beginning and end of the drive segments need to be zero, and limitations on acceleration and jerk due to either vehicle constraints, traffic constraints, or passenger comfort.

Using a discretized version of equation (1) and assuming the energy at the wheel of the vehicle $E_{w,n}$ as shown in (5).

$$E_{w,n} = \frac{m}{2} (v_{n+1}^2 - v_n^2) + \frac{1}{2} C_d A \rho v_n^3 \Delta t + m g f_r v_n \Delta t \quad (5)$$

where n is the index of a discretized time segment. The acceleration of the vehicle is approximated by the difference in kinetic energy at each segment.

The energy at the battery $E_{b,n}$ for forward motion and reverse power flow is then given by (6):

$$E_{b,n} = \begin{cases} \eta_{frrw}(T, \omega)^{-1} E_{w,n} & \text{for } E_{w,n} \geq 0 \\ \eta_{reg}(T, \omega) E_{w,n} & \text{for } E_{w,n} < 0 \end{cases} \quad (6)$$

where $\eta_{frrw}(T, \omega)$ and $\eta_{reg}(T, \omega)$ are the efficiency of the vehicle for forward power flow and reverse power flow, respectively. T is the torque of the motor, and ω is its rotational speed. The efficiency values correspond to the complete powertrain, including the mechanical drivetrain and battery efficiencies which have very little variations under different power levels.

Therefore, by adding all discretized energy segments, the total energy drained from the battery E is given by (7), where N is the final discrete time-segment, i.e., when the vehicle reaches a stop.

$$E = \sum_{n=1}^N E_{b,n} \quad (7)$$

With that, we can then formulate the optimization problem shown in (8).

$$\begin{aligned} \min_{v_n} \quad & \sum_{n=1}^N E_{b,n}, \quad \text{s.t.} \quad \sum_{n=1}^N \frac{v_n}{N} = v_{avg} \\ & 0 \leq v_n \leq v_{max} \\ & d_{max} \leq \frac{v_{n+1} - v_n}{\Delta t} \leq a_{max} \quad \forall n \in \{1, \dots, N-1\} \\ & d_{max} \leq \frac{-v_n}{\Delta t} \leq a_{max} \quad \text{if } n = N \end{aligned} \quad (8)$$

where v_{avg} is the desired average speed, v_{max} is the maximum allowed speed, d_{max} is the maximum allowable deceleration, and a_{max} is the maximum allowable acceleration.

B. Optimization Results for Typical E-Drive

In Table I, the improvements on energy consumption using the optimized trajectory are summarized for a typical torque-speed dependent efficiency characteristic as it was shown in Fig. 4b. Several different vehicles and segment length are compared. Vehicle data can be found in Table II (all vehicle have a coefficient of rolling resistance f_r equal to 0.01).

Fig. 11 shows sample trajectories of speed and cumulative energy expenditure at the battery for a Nissan Leaf (vehicle type 2) and one particular set of conditions, i.e., $v_{avg} = 10\text{m/s}$, $d = 1000\text{ m}$, $a_{max} = 4.6\text{m/s}^2$, $a_{min} = -2\text{m/s}^2$.

One can clearly see that the optimizer expends most energy at the beginning in hard acceleration. After that a sawtooth-like speed trajectory is executed as the optimizer places the trajectory into the high-efficiency region of the torque-speed diagram, which requires higher power levels and cannot be achieved at low constant speeds but by repeated segments of coasting and acceleration. Energy savings of above 50% are not unusual as can be seen in Table I.

TABLE I. ENERGY CONSUMPTION FOR TYPICAL E-DRIVE

Vehicle	Average speed (m/s)	Segment length (m)	Energy utilized (kWs)		Energy saved
			Typical trajectory	Optimal trajectory	
Vehicle type 1	10	300	429.15	226.46	47.23%
		500	649.55	265.02	59.20%
		1,000	913.47	381.62	58.22%
		3,000	2,138.09	1,032.88	51.69%
	18	3,000	3,212.75	1,550.38	51.74%
Vehicle type 2	10	300	247.86	182.74	26.27%
		500	379.84	191.33	49.63%
		1,000	596.89	297.4	50.18%
		3,000	1,571.94	782.98	50.19%
	18	3,000	2,281.56	1,286.24	43.62%
Vehicle type 3	10	300	289.18	162.48	43.81%
Vehicle type 4			390.15	265.63	31.92%
Vehicle type 5			198.48	129.91	34.55%

TABLE II. VEHICLE PARAMETERS UTILIZED IN SIMULATIONS

Vehicle	Mass (kg)	C _d A (m ²)	Max. Accel. (m/s ²)	Max. Decel. (m/s ²)
Vehicle type 1	2,018	0.6720	8	2.5
Vehicle type 2	1,525	0.6583	4.6	2
Vehicle type 3	1,525	0.6583	8	2.5
Vehicle type 4	2,500	0.5000	4.6	2
Vehicle type 5	800	2.0000	4.6	2

In summary, optimizing speed trajectories in stop-to-stop urban traffic can have tremendous efficiency benefits. However, this is only possible if complete situational awareness of traffic in the upcoming drive segment can be attained. Unforeseeable events or incorrect/missing information can drastically reduce the effectiveness of the proposed method.

VI. URBAN PLATOONING

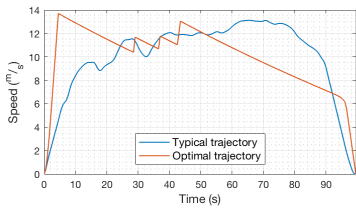
For some time, platooning has been considered to be a promising method for improving efficiency of vehicles driving on highways, especially trucks [11]–[14]. The idea of platooning is to have a train of trucks where one truck follows the next at a close distance, thus, reducing air drag and therefore power and energy/fuel consumption. This effect is especially pronounced at high speeds and close following distances. While close following distances can be problematic, the emerging networked vehicle concept can facilitate relatively safe operation of platooning even at close

following distances. So from an analytical point of view, in highway platooning at constant speeds, one of the four power-consuming terms, i.e. the air drag term, is reduced while rolling resistance, acceleration, and hill-climbing power remain the same.

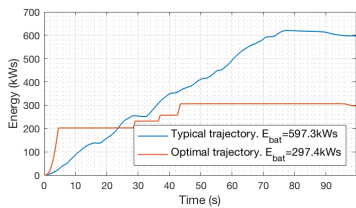
What is proposed in this paper is urban platooning, i.e. vehicles (not necessarily trucks) that execute a speed profile in a platoon formation. The parameters of each vehicle utilized in this simulation are shown in Table III. In contrast to conventional highway platoons, the dynamics of accelerating and decelerating play a key role and the impact of air drag reduction is often negligible since speeds are much lower. In essence, the answer lies in the optimal speed trajectory approach explained in the previous section. For example, if all vehicles are identical, they all have the same energy optimal speed trajectory and can platoon in a rigid platoon. Additional benefits come from the fact that only the lead vehicle needs to have optimization software, traffic can be made more compact, and fast queue depletion due to hard initial acceleration helps decongestion of traffic.

There are essentially two fundamentally different platoon options: One is the case of a rigid platoon where all vehicles execute one common optimal trajectory. The second option is a floating platoon, where vehicles that have similar properties execute their respective optimal trajectories thus drifting apart in a stop-to-stop segment.

Fig. 12 shows the percentage savings (when compared to



(a)



(b)

Fig. 11. Sample trajectories of (a) typical and optimal speed trajectories, (b) cumulative energy consumption over a 1000-meter segment using torque-speed dependent efficiency characteristic.

TABLE III. VEHICLE PARAMETERS UTILIZED IN SIMULATIONS

Vehicle	Mass (kg)	C _d A (m ²)	Max. Accel. (m/s ²)	Max. Decel. (m/s ²)
Vehicle type 1	2,018	0.6720	8	2.5
Vehicle type 2	1,525	0.6583	4.6	2
Vehicle type 3	1,351	0.6998	4.8	2
Vehicle type 4	1,475	0.5600	2	1.5
Vehicle type 5	1,390	0.7140	5	2

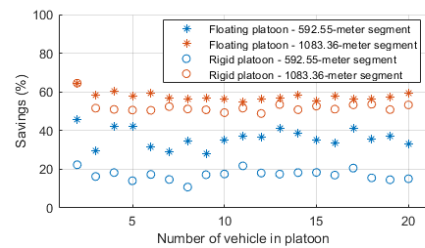


Fig. 12. Percentage of energy saved by floating and rigid platoons of different sizes for a 592.55-meter and a 1083.36-meter segment.

typical speed trajectories) achieved by optimizing two different segments (592.55m and 1083.36m) for each one of the platoon types, i.e., a rigid platoon and a drifting platoon, where the platoon size varies from 2 to 20 vehicles. It can be easily noted that a rigid platoon provides lower savings than a floating platoon. This diminished savings are especially noticed for longer segments. However, rigid platoons are more space-efficient while drifting platoons as the name says will drift apart and care must be taken to avoid collisions. This can be partially addressed by larger initial distances or optimal ordering of vehicles. This, however, results in loss of compactness and bad space utilization. Generally, in contrast to floating platoons, rigid platoons offer great advantages at a relatively low cost for short traffic segments; for long segments, floating platoons are generally more attractive.

Fig. 13a shows the dependency of the energy savings on segment length. Segments varying from 500m to 1000m were tested with an average speed of 10m/s. Similarly, Fig. 13b shows the impact the average speed has on energy savings. The simulation was performed for a segment of 500m with average speed varying from 6 to 11m/s. Each simulation used a platoon of 10 randomly chosen vehicles (from Table III). It is clear that the savings produced by either, individually optimizing each vehicle or optimizing the speed profile for an average vehicle in the platoon maintain relatively constant savings, with little changes based on either the segment length or average speed. Most of the variation observed is due to different arrangements of vehicles.

In all of the above results, efficiency maps based on Fig. 4b were utilized to model the drivetrain efficiency values. In addition, platoon vehicles were randomly generated from the set of vehicles shown in Table III.

VII. CONCLUSION

This paper shows that the confluence of the three concepts (self-driving vehicles, connected vehicles with situational awareness, and e-drives) provides new opportunities with great potential for energy efficiency optimization in several key applications. It is illustrated that in urban transportation, the proposed paradigm can lead to energy savings of over 50% depending on vehicle, infrastructure and traffic parameters. It is shown how one can extend the method to dynamic and stationary platoons of vehicles. Other approaches that boost efficiency by exploiting environmental conditions are also discussed and possible gains are illustrated.

While electric drives can already be found in a small portion of vehicles, the capability of exploiting situational awareness using self-driving capabilities is in its infancy.

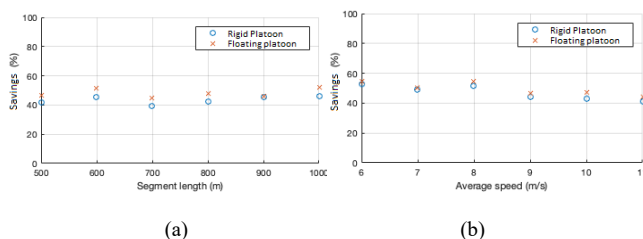


Fig. 13. Percentage of energy saved by 10 randomly chosen vehicles in a platoon (a) for different segment lengths with an average speed of 10m/s and (b) for different average speeds in a 500-meter segment.

Therefore the proposed mechanisms can be realized only in a very small portion of vehicles and in controlled environments such as dedicated lanes, public transport systems, etc. Long term aspects of the proposed paradigm look promising, but a few obstacles need to be overcome: In particular, all examples presented in this paper assumed complete situational awareness. In practice this is not feasible and the longer the time horizon the higher the uncertainty. Even for short time horizons, unexpected events are unavoidable and will reduce the effectiveness of the proposed method. Realization of situational awareness providing apps and the extraction of important data in real-time are also open problems. Also, real-time computation of the optimal trajectory still is a challenging area, but more and more powerful processors in autonomous vehicles will eventually mitigate this problem.

REFERENCES

- [1] A. Sciarretta, G. De Nunzio, and L. L. Ojeda, "Optimal ecodriving control: Energy-efficient driving of road vehicles as an optimal control problem," *IEEE Control Systems Magazine*, vol. 35, no. 5, pp. 71–90, Oct 2015.
- [2] X. Wu, X. He, G. Yu, A. Harmandayan, and Y. Wang, "Energy-optimal speed control for electric vehicles on signalized arterials," *IEEE Transactions on Intelligent Transportation Systems*, vol. 16, no. 5, pp. 2786–2796, Oct 2015.
- [3] S. Mandava, K. Boriboonsomsin, and M. Barth, "Arterial velocity planning based on traffic signal information under light traffic conditions," in *2009 12th International IEEE Conference on Intelligent Transportation Systems*, Oct 2009, pp. 1–6.
- [4] X. Qi, G. Wu, P. Hao, K. Boriboonsomsin, and M. J. Barth, "Integrated-connected eco-driving system for phevts with co-optimization of vehicle dynamics and powertrain operations," *IEEE Transactions on Intelligent Vehicles*, vol. 2, no. 1, pp. 2–13, 2017.
- [5] G. D. Nunzio, C. C. de Wit, P. Moulin, and D. D. Domenico, "Eco-driving in urban traffic networks using traffic signal information," in *52nd IEEE CDC*, Dec 2013, pp. 892–898.
- [6] Z. Yi and P. H. Bauer, "Effects of environmental factors on electric vehicle energy consumption: a sensitivity analysis," *IET Electrical Systems in Transportation*, vol. 7, no. 1, pp. 3–13, 2017.
- [7] M. Ehsani, Y. Gao, and A. Emadi, *Modern Electric, Hybrid Electric, and Fuel Cell Vehicles: Fundamentals, Theory, and Design*, Second Edition, ser. Power Electro and Applic. Series. CRC Press, 2009.
- [8] Z. Yi and P. H. Bauer, "Adaptive multiresolution energy consumption prediction for electric vehicles," *IEEE Transactions on Vehicular Technology*, vol. 66, no. 11, pp. 10515–10525, Nov 2017.
- [9] E. F. Mello and P. H. Bauer, "Energy-optimal speed trajectories between stops," *IEEE Transactions on Intelligent Transportation Systems*, in press.
- [10] Z. Yi and P. H. Bauer, "Energy aware driving: Optimal electric vehicle speed profiles for sustainability in transportation," *IEEE Transactions on Intelligent Transportation Systems*, pp. 1–12, 2018.
- [11] A. A. Alam, A. Gattami, and K. H. Johansson, "An experimental study on the fuel reduction potential of heavy duty vehicle platooning," in *13th International IEEE Conference on Intelligent Transportation Systems*, Sept 2010, pp. 306–311.
- [12] A. Davila. (2013) Report on fuel consumption. SARTRE, Deliverables. [Accessed: Dec. 10, 2018.]. [Online]. Available: <https://www.sp.se/sv/index/research/dependable-systems/Documents/The%20SARTRE%20project.pdf>
- [13] X.-Y. Lu and S. Shladover, *Automated Truck Platoon Control and Field Test*, Road Vehicle Automation. Springer International Publishing, 08 2014.
- [14] M. Hovgard and O. Jonsson, "Energy-optimal platooning with hybrid vehicles," Master's thesis, Chalmers University of Technology, Gothenburg, Sweden, 2017, [Accessed: Dec. 10, 2018.]. [Online]. Available: <http://publications.lib.chalmers.se/records/fulltext/250408/250408.pdf>